OFFICE OF NAVAL RESEARCH

GRANT N00014-89-J-1178

R&T Code 413q001-01

TECHNICAL REPORT NO. 32

A Spectroscopic Differential Reflectometry Study of (100), (110), (111), (311), and (511) Silicon Surfaces

by

S. Chongsawangvirod and E.A. Irene
Department of Chemistry, CB# 3290
University of North Carolina
Chapel Hill, North Carolina 27599-3290

Submitted to the

Journal of Electrochemical Society

CURITY CLASSIFICATION OF THIS PAGE

REPORT DOCUMENTATION PAGE

1. REPORT SECURITY CLASSIFICATION Unclassified	1b. RESTRICTIVE MARKINGS
2. SECURITY CLASSIFICATION AUTHORITY	3. DISTRIBUTION/AVAILABILITY OF REPORT Approved for public release; distribution unlimited.
2b. DECLASSIFICATION/DOWNGRADING SCHEDULE	
4. PERFORMING ORGANIZATION REPORT NUMBER(S) Technical Report #32	5. MONITORING ORGANIZATION REPORT NUMBER(S)
6a. NAME OF PERFORMING ORGANIZATION UNC Chemistry Dept. 6b. OFFICE SYMBOL (If applicable)	7a. NAME OF MONITORING ORGANIZATION Office of Naval Research (Code 413)
6c. ADDRESS (City, State and ZIP Code) CB# 3290, Venable Hall University of North Carolina Chapel Hill, NC 27599-3290	7b. ADDRESS (City, State and ZIP Code) Chemistry Program 800 N. Quincy Street Arlington, Virginia 22217
8a. NAME OF FUNDING/SPONSORING ORGANIZATION Office of Naval Research 8b. OFFICE SYMBOL (If applicable)	9. PROCUREMENT INSTRUMENT IDENTIFICATION NUMBER Grant #N00014 89-J-1176
8c. ADDRESS (City, State and ZIP Code) Chemistry Program 800 N. Quincy Street, Arlington, VA 22217	10. SOURCE OF FUNDING NOS. PROGRAM ELEMENT NO. / PROJECT NO. / TASK NO. / WORK UNIT NO.
11. TITLE (Include Security Classification) A SPECTROSCOPIC DIFFERENTIAL REFLECTOMETRY STUDY OF (100), (110), (111), (311), AND (511) SILICON SURFACES	
12. PERSONAL AUTHOR(S) S. Chongsawangvirod and E.A. Irene	
13a. TYPE OF REPORT Interim Technical 13b. TIME COVERED FROM _____ TO _____	14. DATE OF REPORT (Yr., Mo., Day) December 6, 1990 15. PAGE COUNT 25
16. SUPPLEMENTARY NOTATION The Journal of Electorchemical Society	

17. COSATI CODES			18. SUBJECT TERMS (Continue on reverse if necessary and identify by block number)
FIELD	GROUP	SUB. GR.	

19. ABSTRACT (Continue on reverse if necessary and identify by block number)

Spectroscopic Differential Reflectomety, SDR, has been applied to study differences in silicon surfaces with different crystallographic orientations and with very thin films. The SDR technique measures the normalized difference in reflectance of two adjacent samples in the spectral range of 250-800 nm at near normal incidence. This study demonstrates the surface sensitivity of the SDR technique to the Si crystal orientations, and to the presence of thin oxide films on the Si substrate. The observed orientation dependent spectral features are interpreted in terms of the current understanding of the silicon orientation dependent oxidation kinetics.

20. DISTRIBUTION/AVAILABILITY OF ABSTRACT UNCLASSIFIED/UNLIMITED ☒ SAME AS RPT. ☐ DTIC USERS ☐	21. ABSTRACT SECURITY CLASSIFICATION Unclassified
22a. NAME OF RESPONSIBLE INDIVIDUAL Dr. David L. Nelson	22b TELEPHONE NUMBER (Include Area Code) (202) 696-4410 22c. OFFICE SYMBOL

D FORM 1473, 83 APR EDITION OF 1 JAN 73 IS OBSOLETE.

SECURITY CLASSIFICATION OF THIS PAGE

A SPECTROSCOPIC DIFFERENTIAL REFLECTOMETRY STUDY OF (100), (110), (111), (311), AND (511) SILICON SURFACES

S. Chongsawangvirod and E.A. Irene
Department of Chemistry
University of North Carolina
Chapel Hill, North Carolina 27599-3290

Abstract

Spectroscopic Differential Reflectometry, SDR, has been applied to study differences in silicon surfaces with different crystallographic orientations and with very thin films. The SDR technique measures the normalized difference in reflectance of two adjacent samples in the spectral range of 250-800 nm at near normal incidence. This study demonstrates the surface sensitivity of the SDR technique to the Si crystal orientations, and to the presence of thin oxide films on the Si substrate. The observed orientation dependent spectral features are interpreted in terms of the current understanding of the silicon orientation dependent oxidation kinetics.

Introduction

With recent requirements for MOSFET gate oxide of the order of 10 nm, it is necessary to control the initial stage of Si oxidation which strongly depends on both the silicon surface orientation (1-4) and the surface preparation (5-9). Of particular importance are: the density of silicon atoms on different crystallographic planes (3,4); interface trapped charge where charges may be trapped in surface electronic states (10,11); refractive index

which varies with oxidation conditions and near the interface (12-14); intrinsic film stress which also changes near the interface (15,16); All of these studies indicate that the Si-SiO_2 interface is important in the oxidation kinetics.

In the present study, we investigate the nature of differently oriented single crystal silicon surfaces using an optical reflectance measurement. The reflectance from a semiconductor surface is governed by the interaction of varying energy incident photons with the free and bound electrons. In order to enhance the sensitivity, we utilize Spectroscopic Differential Reflectometry, SDR, which measures the reflectivity difference between two similar samples, rather than the absolute reflectivity. It has been shown that SDR can sensitively monitor thin surface films such as SiO_2 with better than 1 nm resolution (17) as well as the Si surface where damage can be identified near the surface and to tens of nm into the bulk (18,19). In the present study we have examined bare silicon, native oxide covered, and thin purposely grown thermal oxides on differently oriented surface crystal silicon surfaces. Orientation dependent features appear in the SDR spectra, particularly near the silicon interband transitions, and the features are correlated with the silicon oxidation rates, and are found to be independent of the various film growth conditions.

Experimental Procedures

The SDR apparatus used in this study is similar to that originally described by Hummel (20,21), and previously described (17,19) and shown in Figure 1. Unpolarized light from high pressure Xe arc lamp is rastered at near normal incidence across two adjacent similar samples. The reflected light from both samples is detected by the PMT and the

difference in reflectivity, ΔR, is obtained using a lock-in amplifier tuned at the scanning frequency and the average, $\bar{R}$, is obtained via a low-pass filter. The normalized difference in reflectivity, $\Delta R/\bar{R}$, is recorded as a function of wavelength from 250 to 800 nm. Throughout this work we use the (100) Si as the reference, and this orientation is always placed on the right side. For consistency, the lock-in amplifier phase reference is also kept constant for all experiments. Thus we measure $\Delta R/\bar{R}$ as:

$$\frac{\Delta R}{\bar{R}} = \frac{R_{(100)} - R_{(exp)}}{\frac{R_{(100)} + R_{(exp)}}{2}} \qquad (1)$$

where R_{exp} is the sample to be compared with the (100) orientation, and we used commercially available single crystal Si wafers of both n and p type (100), (110), (111), (311), and (511) orientations with resistivities in the 1 to 20 Ω-cm range. No differences were seen for these lightly doped n and p samples, however for very heavily doped Si differences are seen but these experiments are beyond the scope of the present paper. The first three experiments were measured ex-situ in the laboratory ambient. The first set of samples were measured as received from the manufacturers i.e., out from the box and with native oxides. The second experiment was performed after all of the samples were dipped in a concentrated HF (48%) solution for 10s followed by a thorough deionized, D.I., water rinse for 10 min and blow dry in N_2. In the third and fourth experiments prior to the measurement, thin thermal oxides approximately 2 to 2.5 nm were purposely grown on (100), (110), and (111) Si orientations at 1000°C. These samples were first RCA cleaned (22), followed by a 10s dip in HF, and rinsed in D.I. water prior to the thermal oxidation. The

fourth set of samples was measured in-situ in a 500:1/H_2O:HF liquid ambient, where the etch rate was about .2 nm/min. The samples were mounted on a teflon sample holder and placed in a fused silica sample cell. The in-situ sample cell has an optical window perpendicular to the optical axis of the incident beam. The HF solution was introduced through an inlet to begin the etching experiment. During the course of this experiment the thermal oxides on adjacent samples of interest were simultaneously etched back to the silicon interface. Thus yielding bare Si with no surface oxide and without exposing the samples to the laboratory environment. The differential nature of this technique cancels out the effects of experimental environment which in the present case is the etch solution, and thus yields only the difference in reflectance between the two samples. This fourth in-situ experiment was performed in order to eliminate the possibility that the spectral features observed in the first three experiments were due to the oxides.

Results and Discussions

Figure 2 show the normalized difference in reflectivity, $\Delta R/\bar{R}$, as was defined by eqn (1) as a function of wavelength for the different surface orientations relative to the (100) orientation. All the spectra display downward peaks at 292 nm (4.3 eV) and 365 nm (3.4 eV). The two peaks correspond to the direct interband transitions for Si, viz. $L'_3 \rightarrow L_1$ (3.4 eV) and Σ (4.3 eV), i.e. the energies at which the electrons in the valence band are directly excited into the conduction band. It should be noted that whether these peaks are minimum or maximum is adjustable by either reversing the samples from left to right or by shifting the reference phase on the lock-in amplifier by 180^o. There is also a gradually increasing $\Delta R/\bar{R}$

as the wavelength decreases for the comparisons of (311) and (511) orientations.

It was previously shown that light in the wavelength of 200 to 400 nm (6.2 to 3.1 eV), where the interband transitions are observed, penetrates about 10 nm into crystalline Si and amorphous Si (18). Thus, the spectral features for the different surface orientations came from the Si-SiO_2 interface region.

Before attempting to interpret the details of the specific orientation order for the spectra in Fig. 2, it must first be determined whether these spectral difference features are caused by the difference in the Si structure near the surface, the effect of thin films on the different orientations, and/or the surface films themselves.

It is known that oxidation rate of Si is orientation dependent (1-4). Thus different oxide thickness grown under the same conditions is likely and the oxide thickness difference may affect the spectra. Table 1 shows the native oxide thicknesses on all Si orientations in our study. The result shows slightly thicker oxide films on (311) and (511) orientations. To understand the effect on the SDR spectra of thin native oxide film on Si, a calculation was performed using a homogeneous film optical model and literature values for the optical properties of the SiO_2 film (23) and Si substrate (24), and then this result compared with the experimental data is shown in Fig. 3. The thicknesses used in the calculation were 1.9 and 2.8 nm obtained from ellipsometry measurements on the actual samples as in the case of (100) vs (311) orientations respectively. The simulated spectra (dashed line in Fig. 3) shows only a decrease in reflectivity of the thicker oxide sample due to the interference between the incident light and the reflected light at the SiO_2 interfaces. Since the interference effect is a function of both the optical path length through the oxide film and

the wavelength, the effect increases as the wavelength decreases. Plotted along with the calculated spectrum in Fig. 3 is the experimental spectrum (open circles) for the comparison of (100) vs (311) orientations which contains both orientational spectral features and any thickness variation and/or native oxide features. The difference between the experimental and calculated spectra should therefore contain only the orientational spectral features (solid line). Thus, it is shown that orientation dependent features can not be explained simply by a thickness difference variation in the adjacent films.

In order to minimize the native oxide thickness on the Si surfaces, all the samples were dipped in a concentrated HF solution for 10s and then rinsed in D.I. water. The comparison is shown in Fig. 4. Ellipsometry showed 1 nm or about half the original native oxide thickness to be present immediately after the HF dip and D.I. rinse. SDR shows very little difference in the magnitude of the interband transition peaks from this experiment, and although Fig. 4 shows only the comparison of (100) vs (111) orientations, similar behavior is observed for the other orientations.

In order to completely eliminate the surface oxide layer, the comparison measurement was performed in-situ in the HF solution and the results are shown in Fig. 5. It is seen that both 292 and 365 nm peaks remained even when surface oxide films are not present. Recent studies have shown that an HF cleaned Si surface is terminated with hydrogen as well as fluorine atoms (25-30). It is assumed that in the SDR experiment whatever occurs to both samples is eliminated due to the nature of differential technique. Thus the two prominent spectral features observed must be dominated by the differences in the surface orientations. From this we should not conclude that there is no difference

between a native oxide and a thin purposely grown oxide sample. Fig. 6 shows this comparison of two samples on (100) orientations, one with native oxide and the other with thermal oxide with essentially the same oxide thickness. The result shows small peaks at the same critical wavelengths, indicating that there is a difference in the oxide structure and/or there is an effect of the oxide upon the Si atoms near the interface, but this effect while noticeable is minor compared to the larger surface orientation effect seen in Fig. 2.

Finally, it is shown in Fig. 7 that the orientation dependent features are still apparent when thin thermal oxides of about 2.5 nm are grown on the surfaces. These spectral features will be more difficult to discern for longer oxidation times because the $\Delta R/\bar{R}$ will be dominated by the optical interference from thickness differences between the samples obtained from the orientation dependent oxidation rate.

Having eliminated possible extraneous causes of the SDR spectral features we have confidence that there is a surface orientation effect observed in SDR. Fig. 8 shows the SDR data from Fig. 2 but with the thickness variations eliminated, and two observations are made from the data in Fig. 8 and discussed. First, the peak position at both critical wavelengths remain constant within 2 nm for all our experiments. The implication is that the energy at which electrons undergo optical transitions remains constant thus the electronic band structure is unaffected. Secondly, the magnitude of each peak at the critical wavelengths varies as a function of surface orientation as summarized in Table 1. The negative sign for the peak heights means that the reflectivity of all the orientations at the critical wavelengths is greater than the (100) orientation as given by eqn (1). The orientation dependent reflectivity is observed with the order:

$$(111) > (110) > (311) > (511) > (100)$$

This variation observed in $\Delta R/\bar{R}$ is the manifestation of the reflectivity difference among the different Si orientations.

It is known that R is proportional to the complex index, $\tilde{N}$, which in turn depends on the real index, n, and the absorption index, k. It was calculated from eqn (1) that in order for $\Delta R/\bar{R}$ for two adjacent samples to decrease at the critical wavelength as observed in Fig. 8, n, for the sample of interest, must decrease or k must increase or both. It is also given by the Lorentz-Lorentz formula that n is proportional to the density of atoms (31). For the orientations used this order is (1,3)

$$(110) > (111) > (311) > (511) > (100)$$

hence this does not yield the observed order in R, thus k must be controlling R. This is not surprising since the observed downward peaks near the interband transitions are essentially absorption peaks.

In order to obtain a qualitative idea of the effect of k in the near UV - visible energy range, we use the classical Lorentz theory to describe the forced vibrational motion of bound electrons under the influence of an external field assuming that one electron is quasielastically bound to a given nucleus. From this simplistic theory the imaginary part of the complex dielectric function, $\tilde{\epsilon}$, is related to k as: (32)

$$\epsilon_2 = 2nk = \frac{4\pi e^2 N\gamma\omega}{m^2(\omega_0^2-\omega^2)^2+\gamma^2\omega^2} \qquad (2)$$

where N is the number of electrons, ω is the frequency, m is the electron mass, ω_0 is the frequency at which the electron vibrates without an external force, and γ is the damping

constant. From eqn (2) it is seen that the number of electrons is directly proportional to the absorption index and thus is given by the above determined order for the surface reflectivity. It should be noted that this order is also the same as the oxide growth rate for oxide thicknesses greater than several tens of nm. (3).

It has been reported that an enhanced level of electron emission from photonically stimulated oxidation resulted in oxidation rate enhancements (33,34), thereby indicating that electrons can affect the oxidation kinetics. Also, a study of ultra thin (<3 nm) oxide growth kinetics (35) has revealed that a correlation exists between the barrier for the thin oxide growth and the approximately 3 eV barrier for electron emission from the conduction band in Si into SiO_2. An orientation dependence in this data was not clearly established, since it was thought to be within the accuracy of the oxidation data. The present SDR results suggest that if the electron concentration at the Si surface is important in Si oxidation kinetics, the (111) orientation should oxidize the fastest. It was shown that beyond the very initial regime extending to several tens of nm depending on oxidation condition, the (111) orientation dominates the kinetics (1-3). However, in the very initial regime, the (110) orientation was found to oxidize the fastest. Hence, the number of density of Si atoms must dominates in the earliest stage of oxidation. It should be noted that while it is clear that the (110) oxidizes fastest in this regime, a quantitative comparison (35) clearly shows that the atomic number density alone is insufficient to explain the kinetics. It is therefore proposed that the electron availability, largest on the (111) may also play a role. Beyond several tens of nm, the (111) dominates the kinetics. This has been tentatively attributed to the lower stress in oxide grown on the (111) surface (3), thereby enabling more rapid diffusion of

oxidant through the SiO_2 grown on the (111) surface. However, from a careful consideration of the steady state situation likely obtaining during Si oxidation (36), that the interface reaction constant that may be related to the electron availability at the surface (35) cannot be excluded.

Conclusions

The Spectroscopic Differential Reflectometry technique has been shown to be sensitive in revealing difference in reflectivity in the different orientations of Si. In particular, the spectral features at the interband transitions of Si, strongly suggests a relative order for the absorption index, k, and thus number of available electrons as:

$$(111) > (110) > (311) > (511) > (100)$$

which may help to explain the oxidation growth rate of SiO_2 in the thin film regime, as an additional mechanistic parameter along with the dominant Si surface atom density, and then the electron effect dominates in the regime beyond about 25 nm.

Acknowledgement

This research was supported in part by the Office of Naval Research, ONR.

References

1. E.A. Lewis and E.A. Irene, J. Electrochem. Soc., 134, 2332 (1987).
2. H.Z. Massoud, J.D. Plummer, and E.A. Irene, J. Electrochem. Soc., 132, 745, 2685, 2693 (1985).
3. E.A. Lewis, E. Kobeda, and E.A. Irene, in Semiconductor Silicon, p. 416, H.R. Huff, T. Abe, and B. Kolbesen, Editor, Electrochemical Society, NJ (1986).
4. E.A. Irene, H.Z. Massoud, and E. Tierney, J. Electrochem. Soc., 133, 1253 (1986).
5. F.J. Grunthaner and J. Maserjian, IEEE Trans. Nucl. Sic., NS-24, 2108 (1977).
6. F.N. Schwettmann, K.L. Chang, and W.A. Brown, Abstract 276, p. 688, The Electrochemical Society Extended Abstracts, Vol 78-1, Seattle, WA, May 21-26, 1978.
7. G. Gould and E.A. Irene, J. Electrochem. Soc., 134, 1031 (19[illegible]).
8. G. Gould and E.A. Irene, J. Electrochem. Soc., 135, 1535 (1988).
9. D.B. Kao, B.E. Deal, J.M. De Larios, C.R. Helms, in Physics and Chemistry of SiO_2 and the Si-SiO_2 interface, p. 421, C.R. Helms and B.E. Deal, Editor, Plenum Press, New York, N.Y. (1988).
10. R.R. Razouk and B.E. Deal, J. Electrochem. Soc., 126, 1573 (1987).
11. S.C. Vitkavage, E.A. Irene, and H.Z. Massoud, J. Appl. Phys., Accepted for publication (1990).
12. E.A. Taft, J. Electrochem Soc., 125, 968 (1978).
13. E.A. Irene, E. Tierney, and J. Angillelo, J. Electrochem. Soc., 129, 2594 (1982).
14. S. Chongsawangvirod, E.A. Irene, A. Kalnitsky, S.P. Tay, and J.P. Ellul, J. Electrochem. Soc., Accepted for publication (1990).

15. E. Kobeda and E.A. Irene, J. Vac. Sci. Technol. B., 6, 574 (1988).

16. E. Kobeda and E.A. Irene, J. Vac. Sci. Technol. B., 7, 163 (1989).

17. U.S. Pahk, S. Chongsawangvirod, and E.A. Irene, J. Electrochem. Soc., Accepted for publication (1990).

18. R.E. Hummel, Wei Xi, P.H. Holloway, and K.A. Jones, J. Appl. Phys., 63, 2591 (1987).

19. T.M. Burns, S. Chongsawangvirod, J.W. Andrews, E.A. Irene, G. Mcguire, and S. Chevacharoenkul, J. Vac. Sci. Technol B, Submitted for publication (1990).

20. J.A. Holbrook and R.E. Hummel, Rev. Sci. Instrum., 44, 463 (1973).

21. R.E. Hummel, Phys. Stat. Sol. (a), 76, 11 (1983).

22. W. Kern and D.A. Puotinen, RCA Rev., 31, 187 (1970).

23. E.D. Palik, Editor, Handbook of Optical Constants of Solids, Acedemic Press, Orlando, FL (1985).

24. D.E. Aspnes and A.A. Studna, Phys. Rev. B., 27, 875 (1983).

25. E. Yablonovitch, D.L. Allara, C.C. Chang, T. Gmitter, and T.B. Bright, Phys. Rev. Lett., 57, 249 (1986).

26. V.A. Burrows, Y.J. Chabal, G.S. Higashi, K. Raghavachari, and S.B. Christman, Appl. Phys. Lett., 53, 998 (1988).

27. T.Takahagi, I. Nagai, A. Ishitani, H. Kuroda, and Y. Nagasawa, J. Appl. Phys., 64, 3516 (1988).

28. G.T. Duranko, D.J. Syverson, L.A. Zazzera, J. Ruzyllo, and D.C. Frystak, in Physics and Chemistry of SiO_2 and the Si-SiO_2 interface, p. 429, C.R. Helms and B.E. Deal,

Editor, Plenum Press, New York, N.Y. (1988).

29. N. Yabumoto, K. Saito, M Morita, T. Ohmi, Abstract S-F-2, p. 1067, The 22nd Conference on Solid States Device and Material, SSDM, Extended Abstract, Sendai, Japan, August 22-24, 1990.

30. T. Sunada, T. Yasaka, M. Takakura, T. Sugiyama, S. Miyazaki, and M. H se, Abstract S-F-3, p. 1071, The 22nd Conference on Solid States Device and Material, SSDM, Extended Abstract, Sendai, Japan, August 22-24, 1990.

31. G. Lucovsky, M.M. Manitini, J. K. Srivastava, and E.A. Irene, J. Vac. Sci. Technol. B, 5, 530 (1987).

32. R.E. Hummel, Electronic Properties of Materials, (Springer-Verlag, New York, N.Y., 1985), p. 159.

33. E.M. Young and W.A. Tiller, Appl. Phys. Lett., 50, 80 (1987).

34. E.M. Young, Appl. Phys. A, A47, 259 (1989).

35. E.A. Irene and E.A. Lewis, Appl. Phys. Lett., 51, 767 (1987).

36. E.A. Irene and R. Ghez, Appl. Surf. Sci., 30, 1 (1987).

Figure Captions

Figure 1. Block diagram of the Spectroscopic Differential Reflectometry Apparatus

Figure 2. Differential reflectance spectra of the comparison of the (100) orientation with the (111), (110), (311), and (511) Si orientations.

Figure 3. A comparison of orientation dependent spectra of (100) vs (311) orientations (open circles) with a simulated differential reflectance spectrum for two adjacent samples with .9 nm difference in SiO_2 thickness on Si substrates (dashed) and the difference between the experimental and the calculated spectra (solid).

Figure 4. Comparison of HF dipped (100) vs (111) Si orientations (dotted) with the "as-received" sample (solid).

Figure 5. In-situ comparison of (100) vs (111) Si orientations in a 500:1/H_2O:HF liquid ambient.

Figure 6. A comparison of purposely grown thermal oxide with native oxide of similar thickness on (100) Si orientation sample.

Figure 7. A comparison of (111) and (110) vs (100) Si orientations with thin thermal oxide grown on the surfaces.

Figure 8. Differential reflectance spectra showing the comparison of the (100) orientation with the (111), (110), (311), and (511) Si orientations after accounting for the oxide thickness variations.

List of Table

Table 1

Si orientations	Native oxide thickness (nm)
(100)	1.9
(110)	1.9
(111)	1.9
(311)	2.8
(511)	2.2

Table 2

Orientations	Peak Heights at 292 nm	Peak Heights at 365 nm
(111)	-.78	-.46
(110)	-.20	-.26
(311)	-.17	-.22
(511)	-.07	-.07

Peak Heights Relative to (100) Orientation

Spectroscopic Differential Reflectometry

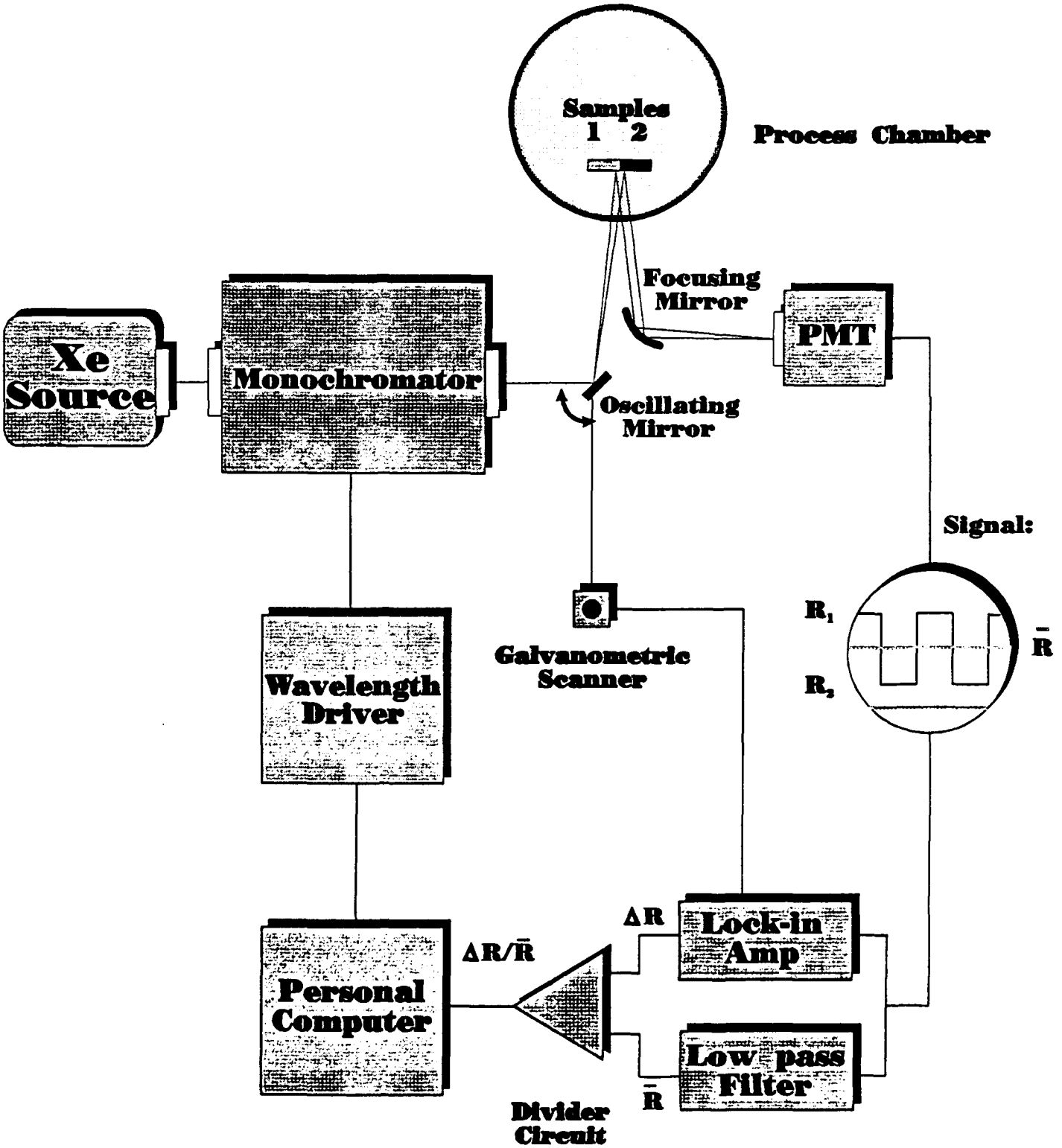

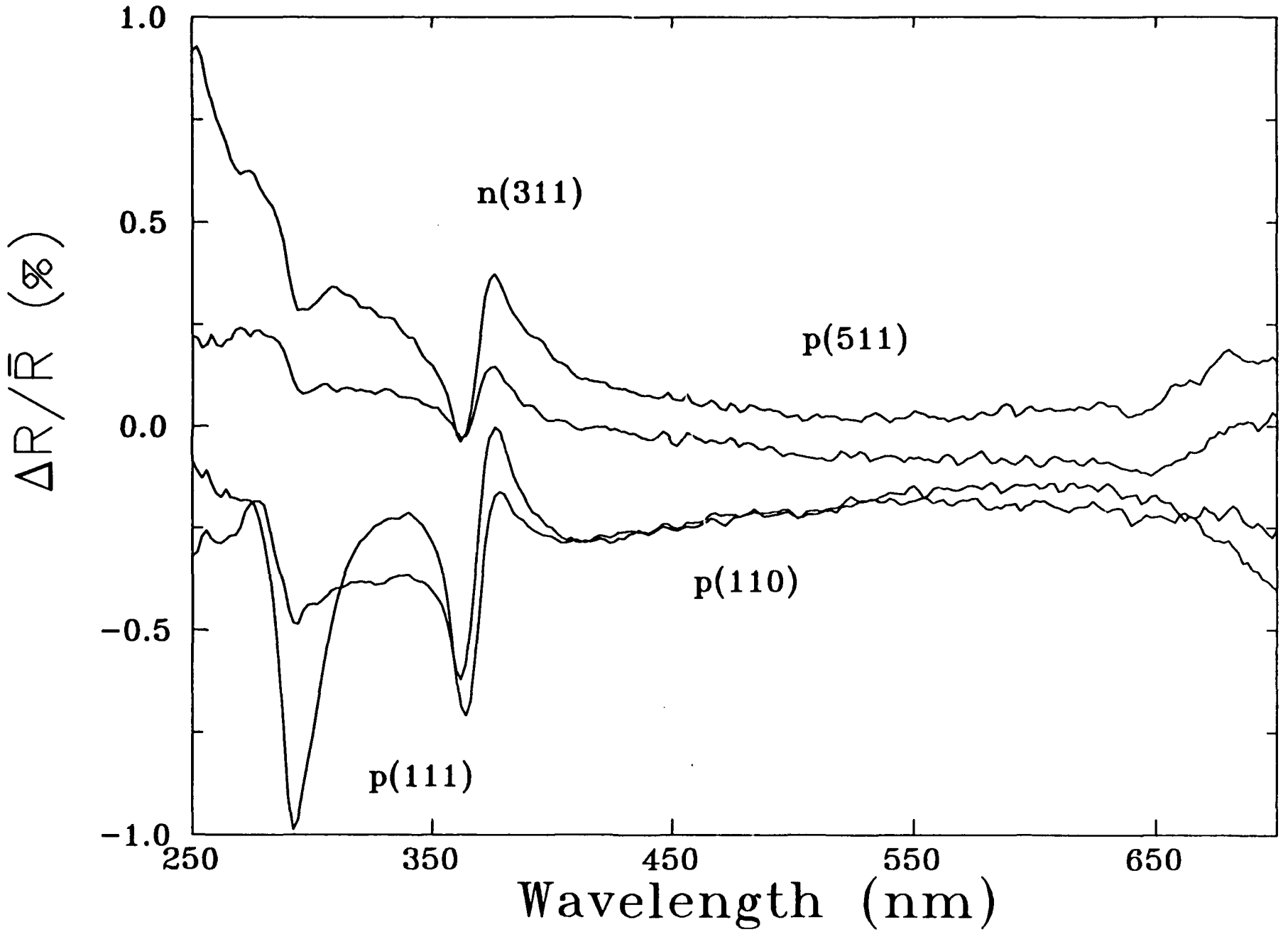
1.0
0.5
0.0
−0.5
−1.0
ΔR/R̄ (%)
n(311)
p(511)
p(110)
p(111)
250
350
450
550
650
Wavelength (nm)

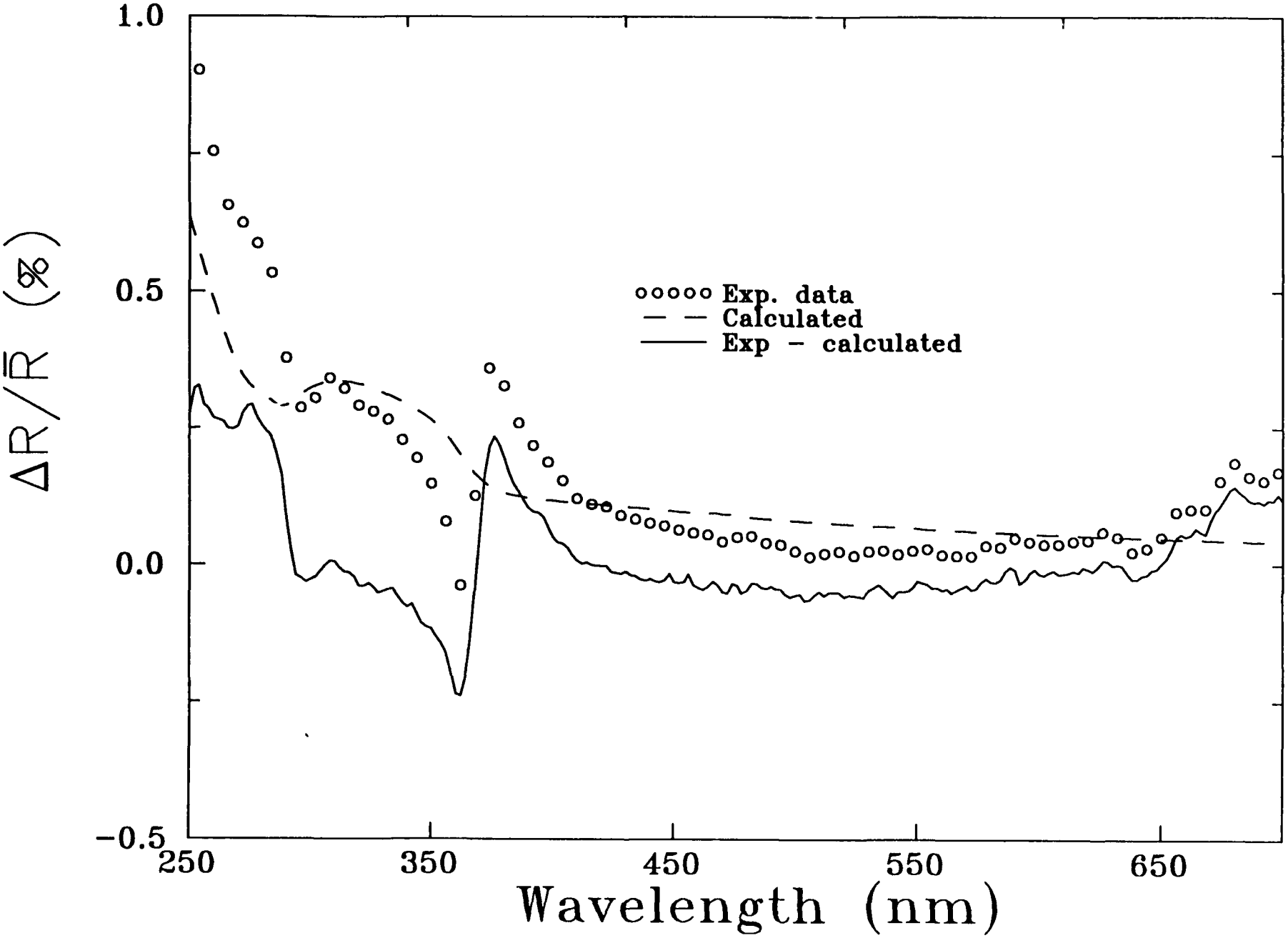
1.0
0.5
0.0
−0.5
250
350
450
550
650
Wavelength (nm)
ΔR/R (%)
Exp. data
Calculated
Exp − calculated

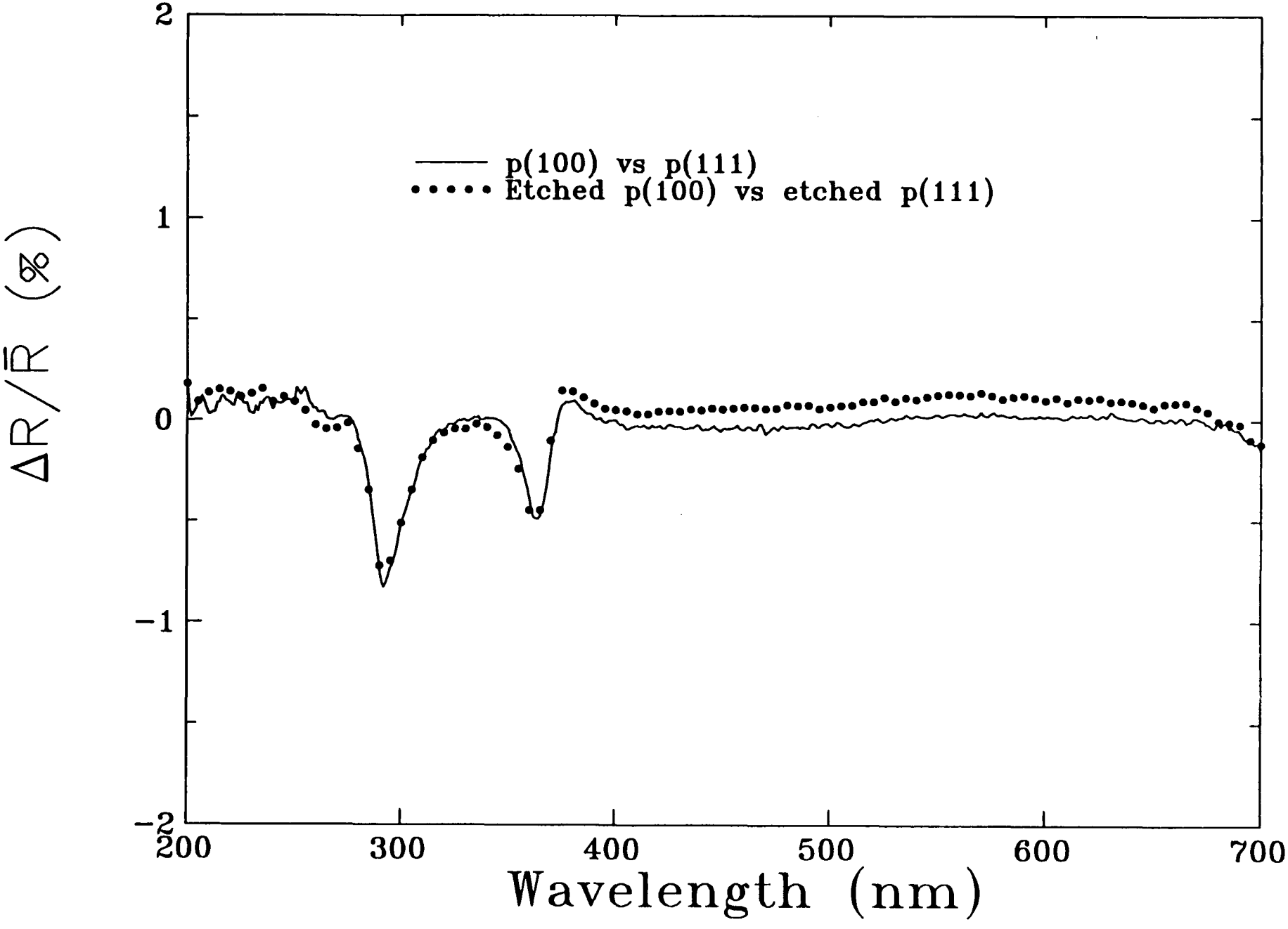
p(100) vs p(111)
Etched p(100) vs etched p(111)
ΔR/R̄ (%)
2
1
0
−1
−2
200
300
400
500
600
700
Wavelength (nm)

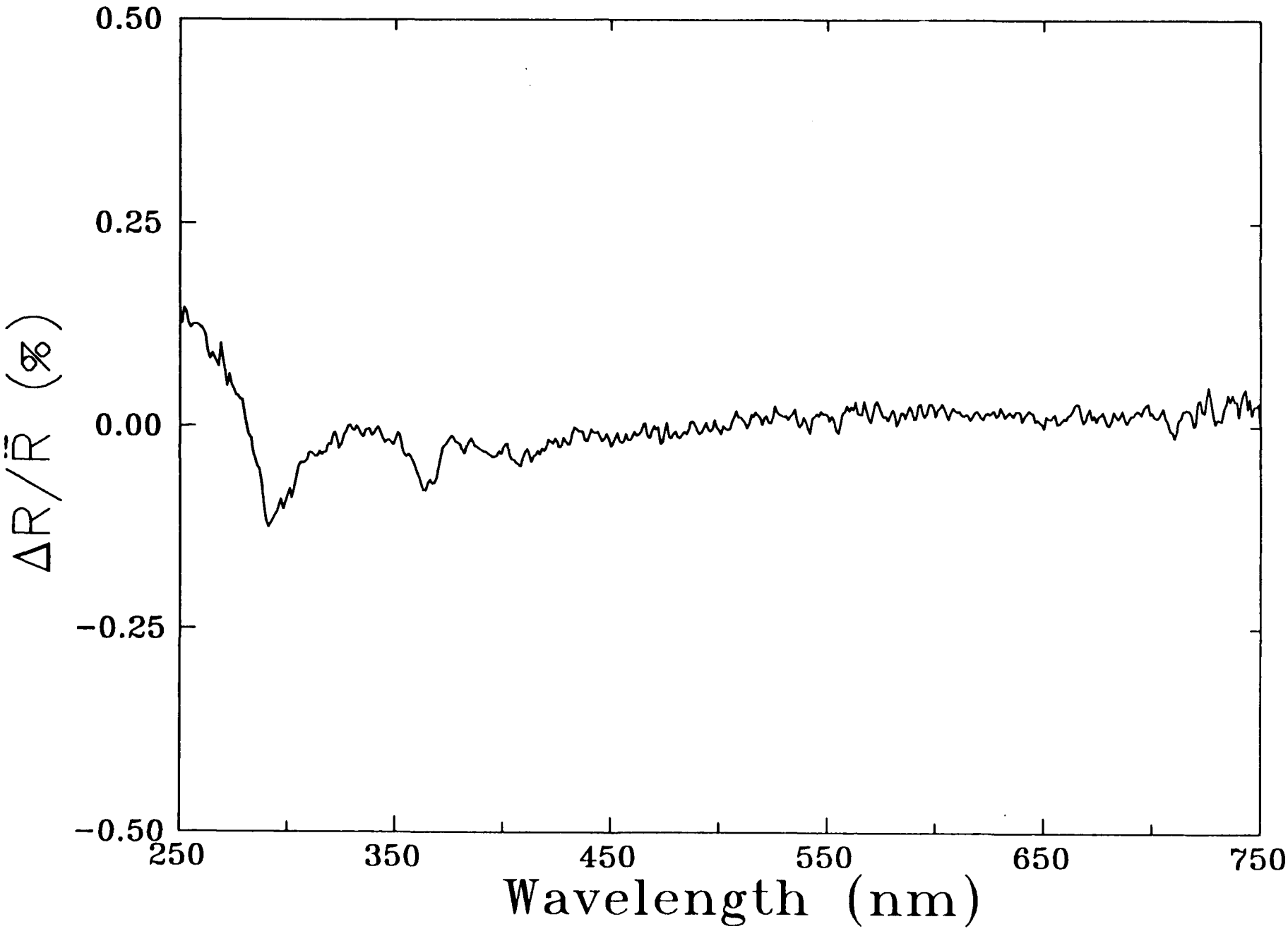
0.50
0.25
0.00
−0.25
−0.50
ΔR/R (%)
250
350
450
550
650
750
Wavelength (nm)

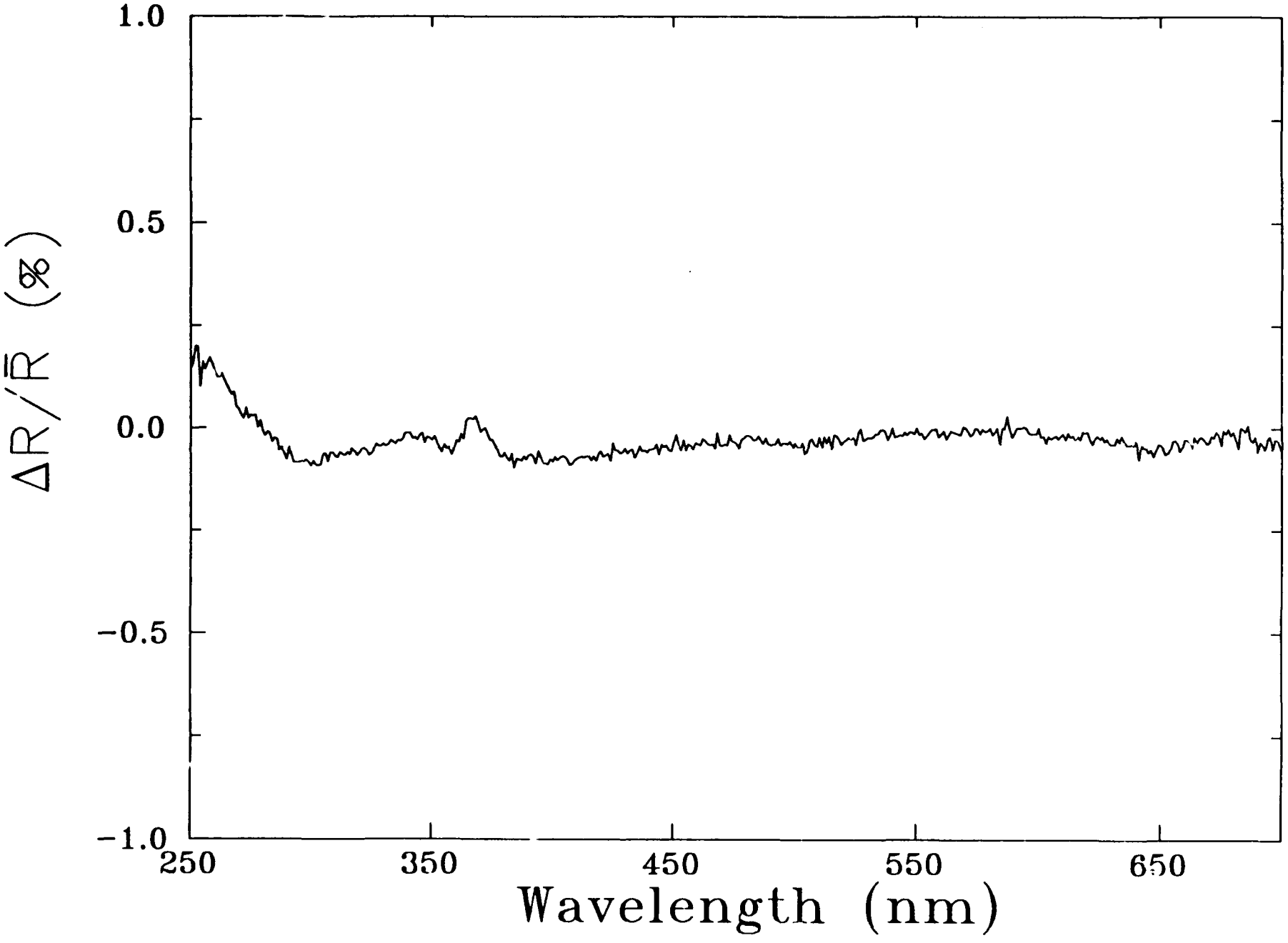
1.0
0.5
0.0
−0.5
−1.0
ΔR/R (%)
250
350
450
550
650
Wavelength (nm)

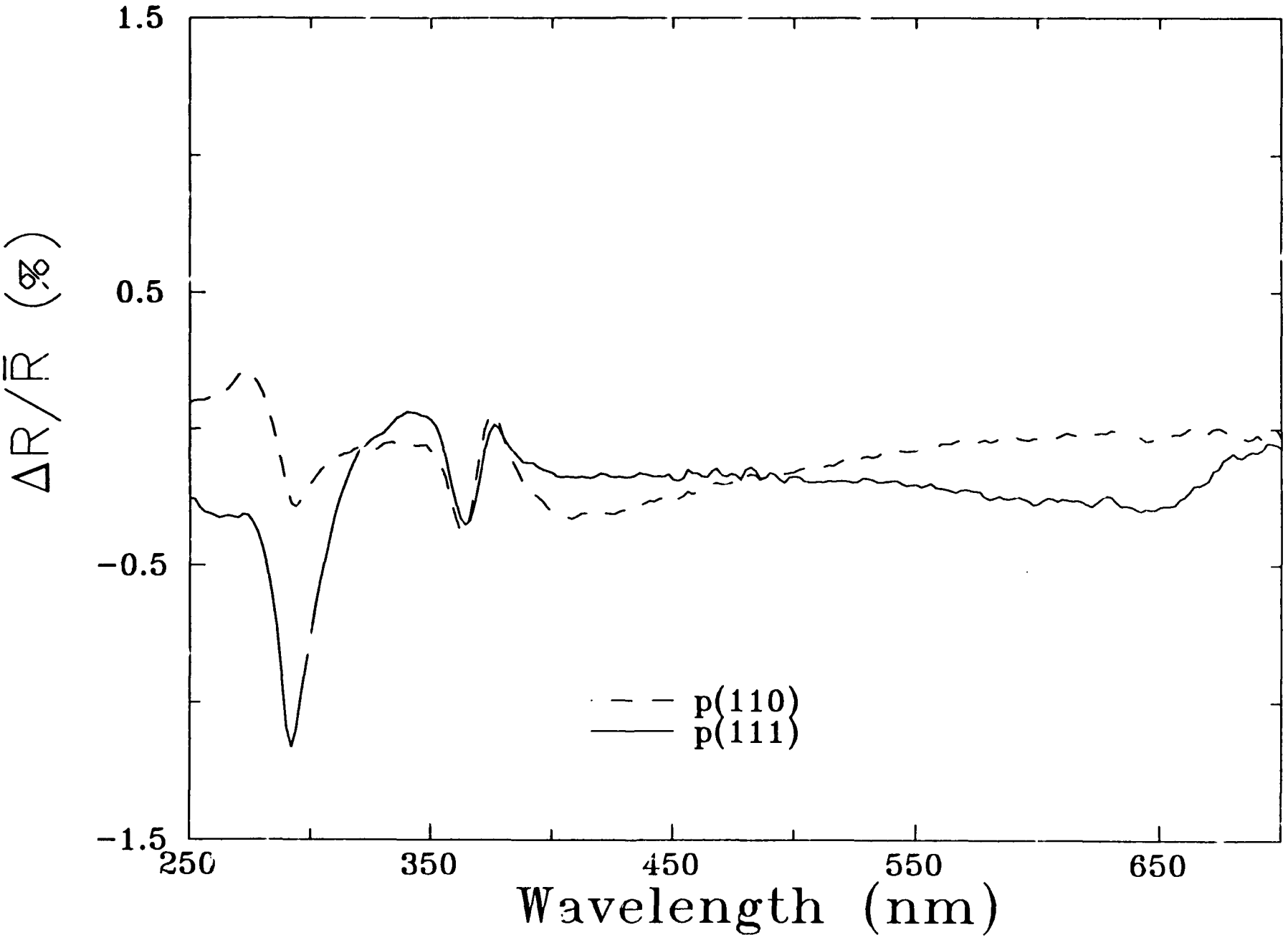
1.5
0.5
−0.5
−1.5
ΔR/R (%)
250
350
450
550
650
Wavelength (nm)
p(110)
p(111)

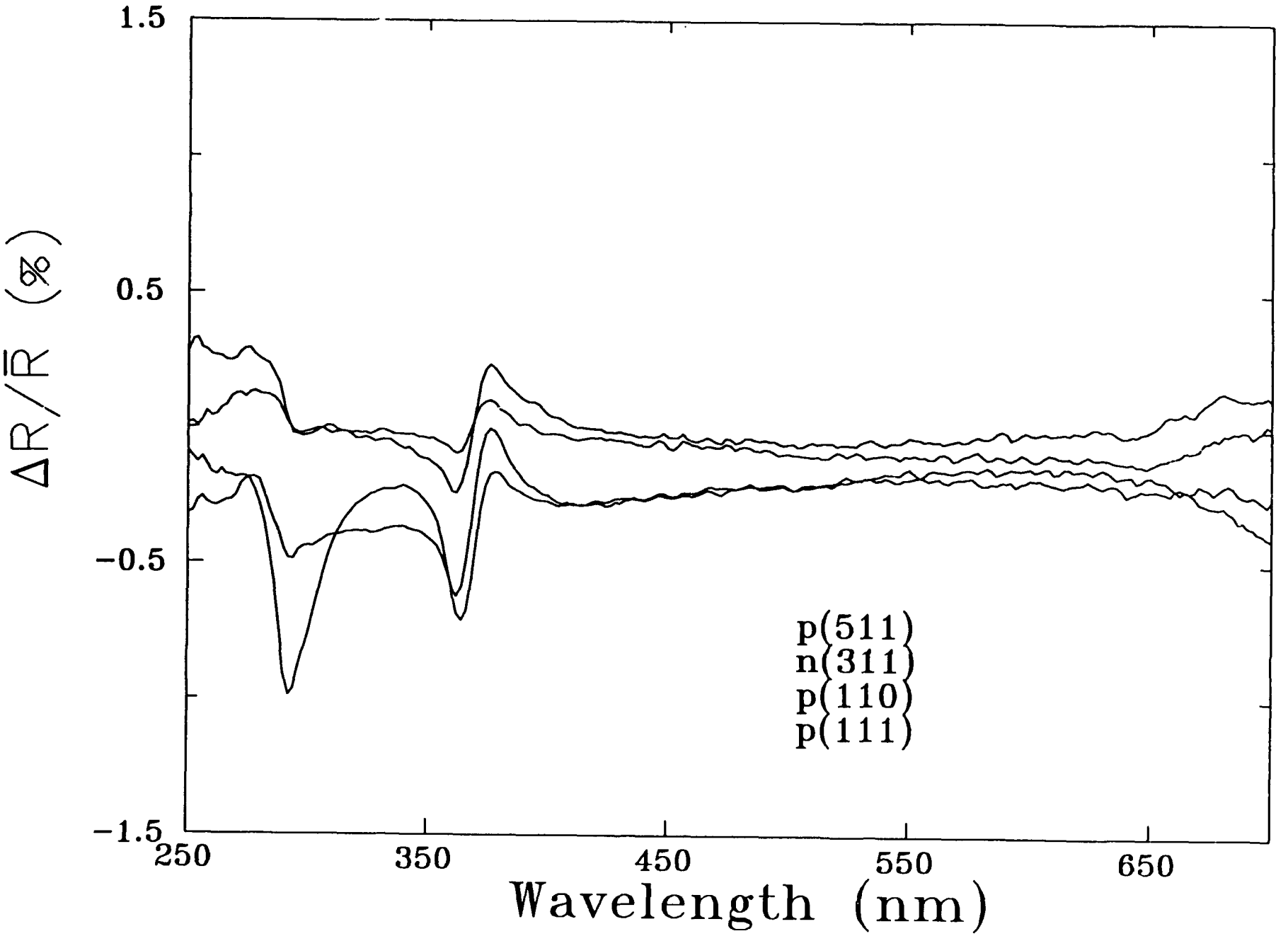
1.5
0.5
−0.5
−1.5
ΔR/R (%)
250
350
450
550
650
Wavelength (nm)
p(511)
n(311)
p(110)
p(111)